$\pi^{\pm}$-p Elastic Scattering at 31.4 MeV

D. E. KNAPP* AND K. F. KINSEY
The University of Rochester, Rochester, New York
(Received 11 March 1963)

Five new measurements of π^-+p and three of π^++p elastic differential cross sections, extend the angular range and the accuracy of the data near 30 MeV. These data, combined with the previous measurements at this energy, provide a significant improvement in the accuracy of s- and nonresonant p-wave phase shifts. A phase-shift analysis yields four solutions, two of which are inconsistent with photoproduction measurements near threshold. One of the remaining two is preferred on the basis of a considerably more likely fit to recent charge-exchange measurements at the same energy. Assuming $f=0.0878$; $\alpha_1=0.087\pm0.009$; $\alpha_{11}=0.051\pm0.008$; $\alpha_{13}=-0.043\pm0.004$; $\alpha_{31}=-0.008\pm0.002$; $\alpha_3=-0.066\pm0.001$.

I. INTRODUCTION

WITH the completion of recent $\pi^-+p\rightarrow\pi^0+n$ charge-exchange measurements near 30 MeV, there existed an extensive set of measurements of pion-proton scattering at this energy.[1–4] However, the phase-shift analysis of these measurements has been disappointing in two respects: First, it has not been possible to obtain a $T=\frac{3}{2}$ phase-shift solution using data at this energy alone, and second, the $T=\frac{1}{2}$ solutions which are obtained contain very large errors.[2,4] The first difficulty will be shown to be characteristic of phase-shift solutions at this energy. The second problem is much improved by the measurements of this paper, which extend the angular range and accuracy of the π^-+p elastic scattering data. We report five measurements of the differential cross section at laboratory angles of 56.4°, 78.7°, 99.8°, 122.8°, and 146.2°. In addition, we report three measurements of the π^++p cross section at 69.5°, 100.1°, and 151.8°, which were made to check consistency with previous measurements.

II. PHYSICAL DESCRIPTION OF EXPERIMENT

A.

The pion beams used in this work were identical to those used for the recent charge-exchange measurements.[4] The same liquid-hydrogen target was also used except for the two backward-scattering measurements for negative pions. For these runs, in the interest of lower background, the outer vacuum walls were moved away from the hydrogen cup so that they could not be seen by both the incident and the scattering telescopes. With this arrangement, the mass of the target walls visible was only 4% of that of the liquid hydrogen in the beam path.

A typical counter arrangement, that of the 56° experiment, is shown in Fig. 1. The incident pions are detected by counters No. 1 and No. 2; scattered pions by counters No. 3 and No. 4. Counter No 5, in anticoincidence, helps to reduce the accidental background counts. A serious source of background at forward angles comes from the muons produced by the decay in flight of the pions. At this energy, these muons occupy a cone of 24° half-angle. Counter No. 6, in anticoincidence, reduced this background by a factor of 10 for the 56° experiment. At other angles, No. 6 was removed and the scattering telescope was placed closer to the target. For the backward angles, the recoil protons were stopped by an absorber placed in front of counter No. 5.

B.

The electronic counting procedures employed the same transistorized modular units used in the charge exchange measurements.[4–6] The assembly of these units for this experiment is shown in Fig. 2. The left-hand, or discriminator branch, selects events on the basis of pulse height and has an 80 nsec resolving time after the discriminators. The right-hand branch selects

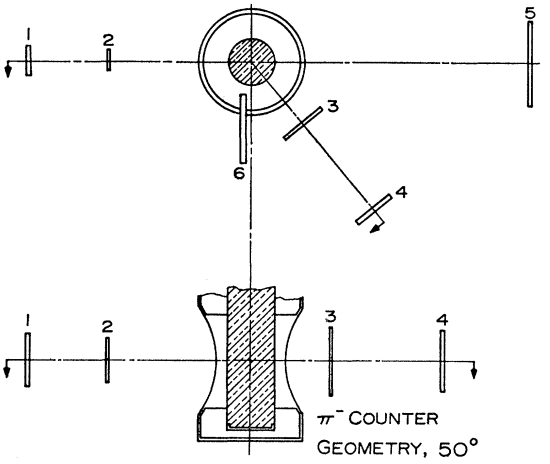

FIG. 1. Counter arrangement for scattering at a nominal angle of 50°. The shaded area is the liquid-hydrogen target.

* Present address: Douglas Aircraft Corporation, Santa Monica, California.

[1] W. B. Johnson and M. Camac, Atomic Energy Commission Report NYO-2169, 1958 (unpublished).

[2] S. W. Barnes, H. Winick, K. Miyake, and K. Kinsey, Phys. Rev. **117**, 238 (1960).

[3] G. Giacomelli, Phys. Rev. **117**, 250 (1960).

[4] K. Miyake, K. F. Kinsey, and D. E. Knapp, Phys. Rev. **126**, 2188 (1962).

[5] R. H. Miller, Rev. Sci. Instr. **30**, 395 (1959).

[6] M. Gettner and W. Selove, Rev. Sci. Instr. **30**, 942 (1959).

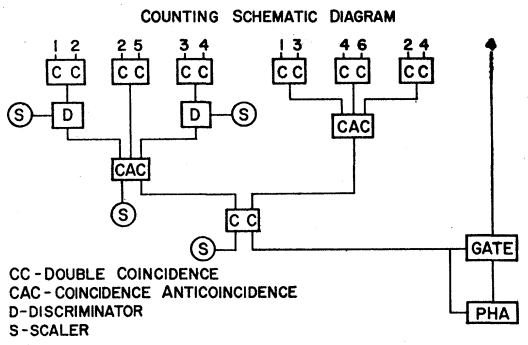

FIG. 2. Block diagram of electronic circuits.

events in fast coincidence with typical resolving times of 7 nsec. Finally, the two branches are joined in a slow coincidence circuit. In addition to the discriminator branch, provision was made for pulse-height analysis of events in the scattering telescope. However, in this experiment, information from pulse-height analysis proved to be of little value in reducing the background of undesired events.

C.

The timing and pulse-height thresholds of the various circuits were set with all of the counters in the incident beam. For counters 3 and 4, the loss of the pion energy from kinematics was simulated by using the appropriate absorbers. The scattering telescope detection efficiency was measured by placing it between counters 1 and 2, the geometry being such that any particle passing through both 1 and 2 must also have passed through 3 and 4.

III. ANALYSIS OF DATA

The analysis of the differential cross-section measurement can best be described by writing the differential cross section in the following way:

$$\frac{d\sigma}{d\Omega}=\frac{N_s}{N_i}\frac{1}{pt\Omega}, \tag{1}$$

where N_i and N_s are the number of incident and scattered particles, p is the number of scattering centers per unit volume, t the target thickness, and Ω the solid angle of the scattering telescope. In the present experiment N_s and N_i are measured directly. The remaining quantities are obtained from the physical dimensions of the scattering geometry and the density of liquid hydrogen.

The major corrections to the measured value of the ratio of scattered to incident particles arise from scattered particles observed when the target is empty, the efficiency for detecting scattered particles, and particles other than pions counted in the incident telescope. These quantities are collected in Table I for the eight measured cross sections. Also shown in Table I is the effective target thickness $\bar{t}$ for each measurement. The effects of a distributed beam, target, and scattering detector are included in an IBM 650 computing program to evaluate this mean thickness and the mean-scattering angle. Minor corrections which have been included are due to gas scattering when the target is empty and to charge-exchange events which are detected in the measurements when the target is full. The angular resolution was between 15° and 20° (full width—half-maximum) for all angles.

TABLE I. The ratio of the scattered- to incident-pion rates is listed for each of the eight measured points. The three major corrections—pions scattered with the target empty, beam purity, and the efficiency for scattered-pion detection—are listed for each point, as is the effective target thickness, $\bar{t}$

Pion	$\theta_{c.m.}$	Full counting rate ($\times 10^6$)	Empty counting rate ($\times 10^6$)	Beam purity (%)	Scattered-particle detection efficiency (%)	$\bar{t}$ (in.)
+	69.5°	8.32	4.13	95.7±0.3	98.3±0.5	1.098
+	100.1°	12.81	4.04	95.7±0.3	98.4±0.5	1.095
+	151.8°	19.87	7.06	95.7±0.3	98.7±0.5	1.096
−	56.4°	5.50	1.73	90.9±1.1	97.9±0.5	1.230
−	78.7°	5.31	1.08	95.4±0.3	98.1±0.5	1.092
−	99.8°	4.08	1.06	95.4±0.3	90.4±0.5	1.127
−	122.8°	3.86	1.67	94.9±0.4	95.5±0.5	1.094
−	146.2°	3.08	1.83	95.4±0.3	97.7±0.5	1.104

These results are combined to give the differential cross sections collected in Table II. The chief factor in the quoted standard deviations is the statistical uncertainty arising from low counting rates. These measurements generally agree with previous results at this energy, but further discussion will be reserved until the phase-shift analysis has been described.

TABLE II. Differential cross-section results.

Pion	$\theta_{c.m.}$	Cross section (mb/sr)	Energy (MeV)
+	69.5°	0.301±0.023	31.4±1.7
+	100.1°	0.609±0.051	31.4±1.7
+	151.8°	1.204±0.052	31.4±1.7
−	56.4°	0.340±0.030	31.9±2.2
−	78.7°	0.259±0.019	31.4±1.8
−	99.8°	0.219±0.017	31.4±1.8
−	122.8°	0.168±0.019	31.4±1.8
−	146.2°	0.11 ±0.018	31.4±1.8

IV. PHASE-SHIFT ANALYSIS

The phenomenological theory of pion-nucleon scattering expressed the cross sections in terms of phase shifts. At low energies the s and p partial waves should be adequate, so a total of 6 phase shifts are introduced, corresponding to the three angular-momentum and two

isotopic-spin states of the system.[7] The phase shifts are calculated from differential cross sections by minimizing the function

$$M=\sum_i \frac{(\sigma_i{}^c-\sigma_i{}^o)^2}{\epsilon_i{}^2}, \tag{2}$$

where $\sigma_i{}^c$ is a cross section expressed in terms of the six phase shifts, $\sigma_i{}^o$ is a measured value with error ϵ_i, and the index i spans all available measurements. The details of this calculation are unchanged from the description by Barnes *et al.*[8] except for the addition of an inner Coulomb correction.[9,10,4]

In order to see why this procedure does not give a solution for the $T=\frac{3}{2}$ phase shifts, it is necessary to evaluate some properties of the M hypersurface. For a function of three variables, the general requirements for a relative minimum are

$$M_{11}>0, \quad \begin{vmatrix} M_{11} & M_{12} \\ M_{21} & M_{22} \end{vmatrix} >0, \quad \begin{vmatrix} M_{11} & M_{12} & M_{13} \\ M_{21} & M_{22} & M_{23} \\ M_{31} & M_{32} & M_{33} \end{vmatrix} >0,$$

where in the case of a $T=\frac{3}{2}$ solution

$$M_{11}=\frac{\partial^2 M}{\partial\alpha_{31}{}^2}, \quad M_{12}=\frac{\partial^2 M}{\partial\alpha_{31}\partial\alpha_3}, \quad M_{13}=\frac{\partial^2 M}{\partial\alpha_{31}\partial\alpha_{33}}, \quad \text{etc.}$$

Using the combined energy phase-shift solutions of Barnes *et al.*[2] these quantities have been evaluated assuming hypothetical experiments of equal weight at 60°, 90°, 120°, and 150°. The first two inequalities are readily satisfied. The third determinant is positive, but is so small that it might readily change sign during the course of an iterative phase-shift analysis. A negative value for this quantity means that the surface has a sort of many-dimensional saddle point. A more detailed investigation using present and earlier $\pi^+ + p$ measurements at 30 MeV shows that the M surface does have a minimum, but that the minimum is so shallow that the errors in phase shifts determined this way are very large. In these circumstances, the most sensible approach seems to be to fix α_{33} from measurements at other energies, since the momentum dependence of α_{33} at low energies is well correlated by the Chew-Low relation,[11]

$$\tan\alpha_{33}=\frac{\frac{4}{3}\eta^3 f^2}{\omega^*(1-\omega^*/\omega_0)}. \tag{3}$$

In fixing α_{33}, values of $\omega^*=2.17$ and $f^2=0.0878$ are used, η being the pion c.m. momentum in units of $m_\pi c$. With α_{33} fixed in this fashion, solutions for α_3 and α_{31} are readily obtained.

Next, the $\pi^- + p$ data were analyzed in terms of the three $T=\frac{1}{2}$ phase shifts, treating the $T=\frac{3}{2}$ phase shifts, previously found, as constants. Solutions were obtained for the present measurements alone, but no solutions were found for the previous $\pi^- + p$ data,[2,3] either separately or in combination with the present measurements. Since the 155° measurement reported in Ref. 2 seemed to disagree with the remainder of the data by about two standard deviations, a solution was attempted omitting this measurement. From a total of eight starting points, chosen to provide a representative variation in α_{11} and α_{13}, four distinct solutions were obtained for the $T=\frac{1}{2}$ phase shifts. These solutions are listed in Table III.

TABLE III. $T=\frac{1}{2}$ solutions.

Solution	α_1	α_{11}	α_{13}	M
I	0.0890	−0.0337	0.0008	0.012
II	0.0878	0.0490	−0.0411	0.018
III	0.0391	−0.0357	0.0311	0.003
IV	−0.0282	−0.0956	−0.0320	3.61

A reasonable criterion for a phase-shift solution at low energy is the quantity $(\alpha_1-\alpha_3)/\eta$, extrapolated to zero-pion energy. This quantity can also be deduced from the Panofsky ratio and from photoproduction experiments near threshold, giving a value 0.245 ±0.010.[9] Even allowing for a deviation of the momentum dependence of the s-phase shifts from the linear (i.e., $\alpha_i=a_i\eta$) as suggested by some authors, solutions III and IV are in evident disagreement with the other low-energy pion data, and are rejected on these grounds.

Finally, 5 parameter solutions were made of all of the elastic scattering data from this laboratory (except the 155° point mentioned above). Only α_{33} was fixed by data at other energies. Again, solutions I and II were found. (See Table IV.)

It is interesting to note that solutions converging to either I or II showed significant changes only in α_{11} and α_{13}. Furthermore, the variation in α_{11} and α_{13} proceeded close to the line $2\alpha_{13}+\alpha_{11}=$ const. Figure 3 shows a cut in the hypersurface M along this line. This is suggestive

TABLE IV. Five-parameter solutions at 31.5 MeV.

	Solution I	Solution II
α_1	0.0889±0.0085	0.0874±0.0089
α_{11}	−0.0368±0.0079	0.0511±0.0077
α_{13}	0.0022±0.0041	−0.0427±0.0044
α_{31}	−0.0082±0.0018	−0.0082±0.0018
α_3	−0.0657±0.0013	−0.0657±0.0013
M	6.46	6.46

[7] H. A. Bethe and F. deHoffmann, *Mesons and Fields* (Row, Peterson, and Company, Evanston, Illinois), Vol. II, p. 63.
[8] S. W. Barnes, B. Rose, G. Giacomelli, J. Ring, K. Miyake, and K. Kinsey, Phys. Rev. **117**, 226 (1960).
[9] J. Hamilton and W. S. Woolcock, Phys. Rev. **118**, 291 (1960).
[10] H. J. Schnitzer (private communication).
[11] G. Chew and F. Low, Phys. Rev. **101**, 1570 (1956).

of the sign ambiguity, where two solutions α_i and α_i' are equivalent if α_i and α_i' are related as (see Ref. 7, p. 73.)

$$2\alpha_{13}'+\alpha_{11}'=2\alpha_{13}+\alpha_{11},$$
$$\alpha_{11}'-\alpha_{13}'=\alpha_{13}-\alpha_{11}.$$

The second relation, however, is not particularly well satisfied.

The charge-exchange data mentioned earlier provide a way to choose between solutions I and II. M was calculated for the combined elastic and charge exchange data for the two solutions. Interpreting M as a χ^2 distribution, solution II has χ^2 probability of 60%, while that of solution I is less than 0.1%. The limited capacity of the 650 precluded a full analysis of the data. The differential cross sections computed from solution II are shown in Fig. 4, along with the present experimental points.

The error matrix for solution II is given in Table V. The total cross sections in mb/sr and scattering amplitudes in units of $\hbar/m_\pi c$ calculated from solution II are

$$\sigma^{++}=6.15\pm0.12, \qquad D_b{}^{+}=0.0349\pm0.0032,$$
$$\sigma^{-0}=7.02\pm0.22, \qquad D_b{}^{-}=0.069\pm0.012,$$
$$\sigma^{--}=1.847\pm0.080.$$

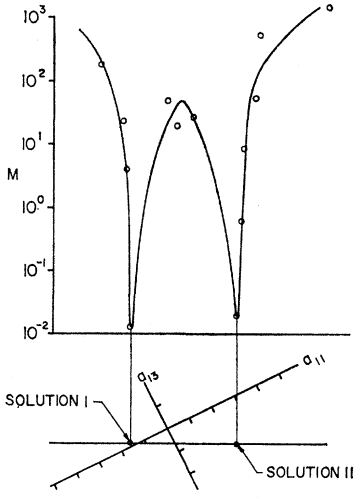

FIG. 3. M values for solutions lying along the line $2\alpha_{13}+\alpha_{11}=$const.

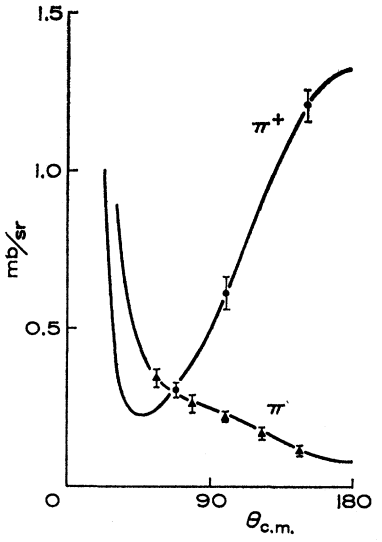

FIG. 4. 4 differential scattering cross sections predicted from solution II phase shifts. Experimental points from this paper are shown.

TABLE V. Error matrix for solution II.

	α_1	α_{11}	α_{13}	α_{31}	α_3	f^2
	80.6	−64.3	36.2	0.379	−0.327	0
		60.4	−75.5	−4.702	0.392	0
$E_{rs}=10^{-6}\times$			19.3	0.026	−0.001	0
				3.36	−0.744	0
					1.88	0
						1.96

ACKNOWLEDGMENTS

The authors wish to express their appreciation for the good counsel and encouragement of Professor S. W. Barnes. Dr. K. Miyake and A. Wieber provided significant aid during the initial phases of the experiment. The operating and technical staff of the 130-in. Cyclotron Laboratory provided their usual high level of support during the experiment. One of us (D.E.K.) held an Eastman Kodak predoctoral fellowship during a portion of the work and was supported in part by the Douglas Aircraft Company, Inc.